Estimating the correlation length of inhomogeneities in a polycrystalline material

Igor Simonovski*, Marko Kovač, Leon Cizelj

Jožef Stefan Institute, Reactor engineering division, Jamova 39, 1000 Ljubljana, SI-Slovenia

* *Corresponding author:*

Tel.: +386-1-5885290

Fax: +386-1-5612335

E-mail: igor.simonovski@ijs.si

Abstract:

This paper deals with the correlation length estimated from a mesoscopic model of a polycrystalline material. The correlation length can be used in some macroscopic material models as a material parameter that describes the internal length. It can be estimated directly from the strain and stress fields calculated from a finite-element model, which explicitly accounts for the selected mesoscopic features such as the random orientation, shape and size of the grains. A crystal plasticity material model was applied in the finite-element analysis.

Different correlation lengths were obtained depending on whether the strain or the stress field was used. The correlation lengths also changed with the macroscopic load. If the load is below the yield strength the correlation lengths are constant, and are of the order of the average grain size. The correlation length can therefore be considered as an indicator of first plastic deformations in the material. Increasing the load above the yield strength creates shear bands that temporarily increase the values of the correlation lengths calculated from the strain fields. With a further load increase the correlation lengths decrease slightly below the average grain size. If displacement boundary conditions are used, the correlation length calculated from strain field is lower then the one calculated from the stress field. The opposite is true, if stress boundary conditions are applied. However, with the exception of the load region where significant shear bands appear, both seem to follow similar qualitative rules.

Keywords: Correlation length; Polycrystalline material; Crystal plasticity;

1 INTRODUCTION

In state-of-the-art structural and stress analyses it is normal to assume that the materials under test are homogeneous and isotropic. Such assumptions are valid for the load-carrying capacities and lifetime analyses of moderately deformed parts that are significantly larger than the inhomogeneities, such as grains, voids or inclusions, which constitute the material. The grains in metals, for example, are typically of the order of 10^{-5} m. Material inhomogeneities may, however, become important when analyzing the following: small parts with sizes similar to the inhomogeneities [1-4], parts subject to a load approaching their strength limit [2,5-7] and the initiation and propagation of short cracks [8-12]. In such cases the localized stress and strain peaks caused by the inhomogeneities usually dominate the response of the material and this may severely limit the applicability of state-of-the-art engineering structural and stress analyses.

A number of attempts to include the inhomogeneities in the models used to describe materials can be found in the literature. In this paper we have defined two, somewhat arbitrary, classes of models:

(1) Advanced macroscopic material models. This group includes, among others, gradient theories [13-15], continuum damage models [16,17] and stochastic finite-element approaches. A common feature of these models is that a more or less explicit model of the inhomogeneities is employed to predict the behavior at the macroscopic (engineering) level. This again tends to require assumptions that lead to the need for additional material parameters, which may require a number of expensive additional tests. Typically, the internal length representing the size of the inhomogeneities is one of the most important material parameters.

(2) Multi-scale models. These explicitly model at least the mesoscopic inhomogeneities (e.g., grain structure, for a review see [18]), while very general and relatively free of assumptions about homogeneities is computationally very demanding and not yet suitable for engineering analyses.

The most efficient way to improve engineering analyses is, therefore, a combination of both these approaches. A very promising way seems to be to employ a multiscale approach in the first step, in order to derive mesoscopic (i.e. on the scale of the grains in the material) stress and strain fields. A statistical analysis of such fields is then used in the second step to derive the correlation lengths. These in turn may be used as a direct input for a stochastic finite-element analysis, which represents the third step. A number of authors have dealt with the third step: see, for example, [19-23]. To the best of our knowledge, however, the first two steps have not yet been treated.

The main goal of this paper is, therefore, an estimation of the correlation lengths within the stress and strain fields of a mesoscopic model of a non-homogenous and anisotropic steel structure. The first part of the paper briefly explains the basic ideas of the mesoscopic model and the procedure employed to derive the correlation lengths. This is followed by a numerical example, which outlines and discusses the most important results – the changes in the correlation lengths with the increase of the remote load, the distribution of the correlation lengths, and the effect of the boundary – and the conclusions.

2 MODEL DESCRIPTION

The estimation of the correlation lengths is based on a mesoscopic material model [18] that includes grains of random size, shape and orientation. The finite-element method [24] is employed to determine the strain and stress fields resulting from a remote load. These two fields are then used for the estimation of the correlation lengths. Strain and stress fields were chosen for this analysis for two main reasons: (1) they can be treated as primary variables and (2) they offer a reasonably good framework for the interpretation of the results. For derived quantities, e.g. Young's modulus [25], the calculation of the correlation lengths is relatively straightforward, however, we did not investigate this here.

2.1 Boundary conditions

Displacement and stress type boundary conditions were investigated, Figure 1. These two boundary conditions are used because they produce the upper and lower limit of the macroscopic equivalent stress at a certain macroscopic equivalent strain. For displacement boundary conditions tensile remote loads with zero shear tractions are applied on the right and top edge. The right edge is only allowed to move parallel to the left edge. Similarly, the top edge is only allowed to move parallel to the bottom edge. Stress boundary conditions are similar to the displacement boundary conditions with the exception that the right and top edge are not required to move parallel to the left and bottom edges.

2.2 Voronoi tessellation

The main idea of the mesoscopic model [18] is to divide the continuum into a set of randomly sized, shaped and oriented subcontinua, i.e. grains. Grains are generated with the Voronoi tessellation [26]. A Voronoi tessellation represents a cell structure constructed from Poisson points by introducing planar cell walls perpendicular to the lines connecting neighboring Poisson points. This results in a set of convex polygons embedding the Poisson points. The polygons completely fill up the underlying space, and each grain is assumed to behave as a continuum. The number of Poisson points is selected in such a way that the obtained average grain size is as close as possible to the average grain size of the used material (0.023 mm). A number of tessellations were generated and a case most suitable for finite element meshing was selected. The details on the Voronoi tessellations are given in Table 1. Two different Voronoi tessellations used in this investigation are presented in Figure 1.

2.3 Material model

The material orientations, which are defined by the orientations of the crystal lattices, are kept constant within a single grain; however, they vary according to a uniform distribution between the grains. Each grain is further subdivided into 8–node, quadratic, reduced-integration and plane strain finite elements. The material orientations are shown with local coordinate systems. Anisotropic elasticity and crystal plasticity [18,27,28] material models were applied. The crystal plasticity model assumes that plastic deformation takes place via a simple shear on a specified set of slip planes. The

slip planes are defined by the random material orientations, which differ among the grains.

2.3.1 Elasticity

The constitutive relations in linear elasticity are given by the generalized Hooke's law

$$\sigma_{ij} = C_{ijkl} \cdot \varepsilon_{kl} \ , \tag{1}$$

where σ_{ij} represents the second-rank stress tensor, C_{ijkl} the fourth-rank stiffness tensor and ε_{ij} the second-rank strain tensor. The material parameters for the 22 NiMoCr 3 7 steel were obtained from the literature for an α-Fe body-centered cubic crystal [29].

2.3.2 Crystal Plasticity

The plastic deformation in monocrystals is assumed to take place via a simple shear on a specific set of planes. The combination of a slip plane, denoted by its normal $m_i^{(\alpha)}$, and a shearing direction, $s_i^{(\alpha)}$, is called a slip system, (α). The plastic deformation rate, $\dot{u}_{i,j}^{p}$, due to a crystallographic slip can be written as [30]

$$\dot{u}_{i,j}^{p} = \sum_{\alpha} \dot{\gamma}^{(\alpha)} s_i^{(\alpha)} m_j^{(\alpha)} , \tag{2}$$

where the summation is performed over all active slip systems, (α), while $\dot{\gamma}^{(\alpha)}$ represents the shear rate. From the well-known relation for strain, $\varepsilon_{ij} = 0.5(u_{i,j} + u_{j,i})$, one can obtain the rate of plastic deformation:

$$\dot{\varepsilon}_{ij}^{p} = \sum_{\alpha} \frac{1}{2} \dot{\gamma}^{(\alpha)} \left(s_i^{(\alpha)} m_j^{(\alpha)} + s_j^{(\alpha)} m_i^{(\alpha)} \right) \ . \tag{3}$$

The constitutive relation of the elastic–plastic monocrystal is now given in terms of stress and strain rates as:

$$\dot{\sigma}_{ij} = C_{ijkl} \cdot \left(\dot{\varepsilon}_{kl} - \dot{\varepsilon}_{kl}^{p} \right). \tag{4}$$

It is assumed that the shear rate $\dot{\gamma}^{(\alpha)}$ depends on the stress only via the Schmid resolved shear stress. This is a reasonable approximation at room temperature and for ordinary strain rates and pressures [30]. The Schmid resolved shear stress for a given slip system is given by eq. (5), while its relationship with the slip rate is given by eq. (6). Yielding is then assumed to take place when the Schmid resolved shear stress exceeds the critical shear stress

$$\tau^{(\alpha)} = s_{i}^{(\alpha)} \sigma_{ij} m_{j}^{(\alpha)}, \tag{5}$$

$$\dot{\gamma}^{(\alpha)} = \dot{a}^{(\alpha)} \left(\frac{\tau^{(\alpha)}}{g^{(\alpha)}} \right) \left(\left| \frac{\tau^{(\alpha)}}{g^{(\alpha)}} \right| \right)^{n-1}. \tag{6}$$

In eq. (6) $\dot{a}^{(\alpha)}$ represents the reference strain rate, n the strain-rate-sensitivity parameter and $g^{(\alpha)}$ the current strain-hardened state of the crystal. In the limit, as n approaches infinity, this power law approaches that of a rate-independent material. The current strain-hardened state $g^{(\alpha)}$ can be derived from:

$$\dot{g}^{(\alpha)} = \sum_{\beta} h_{\alpha\beta} \dot{\gamma}^{(\beta)}, \tag{7}$$

where $h_{\alpha\beta}$ are the slip-hardening moduli. The self-hardening moduli $h_{\alpha\alpha}$ are defined with eq. (8) [31]:

$$h_{\alpha\alpha} = h(\gamma) = h_0 \operatorname{sech}^2 \left| \frac{h_0 \gamma}{\tau_S - \tau_0} \right|, \tag{8}$$

where h_0 is the initial hardening modulus, τ_0 the yield stress (equal to the initial value of the current strength $g^{(\alpha)}(0)$), τ_S the break-through stress where large plastic flow initiates and γ the cumulative slip defined as:

$$\gamma = \sum_{\alpha} \int_{0}^{t} \left| \dot{\gamma}^{(\alpha)} \right| dt, \tag{9}$$

$$h_{\alpha\beta} = q\,h(\gamma)\ ,\ (\alpha \neq \beta). \tag{10}$$

The latent-hardening moduli $h_{\alpha\beta}$ are given by eq. (10), where q is a hardening factor. The material parameters for plasticity are: n = 50, $\mathring{a}^{(\alpha)}$ = 0.001, h_0 = 70 MPa, τ_S = 15.5 MPa, τ_0 = 155 MPa, q = 1.0. A detailed explanation of the parameters can be found in [16].

3 CORRELATION LENGTH

The computational effort needed for the calculation of the stress and strain fields using the crystal-plasticity material model is large, and so this limits the size of the models to approximately 0.40 mm by 0.28 mm. The computational effort could be reduced if just the essential inhomogeneities were taken into the account, and then this information used in a macroscopic model. One way of estimating the essential inhomogeneities is to calculate the domain of influence of the grains. In this study the correlation length is taken as a measure of the domain of influence of the individual grains.

The autocorrelation function $R_{xx}(l_1,l_2)$ of a random process $x(l)$ is defined by eq. (11), where $E[]$ represents the mathematical expectation and $f_{x(l_1)x(l_2)}$ the joint probability-density function. The covariance function $K_{xx}(l_1,l_2)$ of a random process $x(l)$ is defined by eq. (12), and can be expressed using the autocorrelation function, eq. (13).

$$R_{xx}(l_1,l_2) = E[x(l_1)\cdot x(l_2)] = \int\int x_1 \cdot x_2 \cdot f_{x(l_1)x(l_2)}(x_1,x_2)\cdot dx_1 \cdot dx_2\ , \tag{11}$$

$$K_{xx}(l_1,l_2) = E[\ \ (\ x(l_1) - E[x(l_1)]\ )\cdot(\ x(l_2) - E[x(l_2)]\ )\ \ ], \tag{12}$$

$$K_{xx}(l_1,l_2) = R_{xx}(l_1,l_2) - E[x(l_1)]\cdot E[x(l_2)]. \tag{13}$$

For stationary random processes the joint probability-density function $f_{x(l_1)x(l_2)}$ depends only upon the difference l_2-l_1. Consequently, the autocorrelation and covariance functions also depend only on the difference l_2-l_1. If, in addition to the stationarity, the average value of the random process is zero, then the autocorrelation and covariance functions of the process involved are equal: see expressions (14) and (15).

$$R_{xx}(l_1,l_2)=R_{xx}(0,l_2-l_1)=R_{xx}(l_2-l_1)=R_{xx}(l), \qquad l=l_2-l_1, \tag{14}$$

$$K_{xx}(l)=K_{xx}(l_2-l_1)=R_{xx}(l)-\underbrace{E[x(0)]}_{=0}\cdot\underbrace{E[x(l_2-l_1)]}_{=0}=R_{xx}(l). \tag{15}$$

For covariance functions of the form given by the equation (16), the correlation length λ can be defined as the value of the parameter l for which the envelope of the covariance function falls to the value $K_{xx}(0)/e$, Figure 2.

$$K_{xx}(l)=K_{xx}(0)\cdot e^{-|l|/\lambda}\cdot\cos(\omega\cdot l). \tag{16}$$

Now, let us assume that we have a vector of data **g** for which we want to determine the correlation length. First, the autocorrelation function is estimated using the discrete correlation theorem, eq. (17). In eq. (17) the symbol G_k represents the discrete Fourier transformation of the vector **g**, while the symbol * stands for the complex conjugation. We calculate the discrete Fourier transform of the vector **g** to obtain G_k. Next, we multiply, index by index, the vector G_k by G_k^*. Finally, we calculate the inverse Fourier transform of the product $G_kG_k^*$ to determine the autocorrelation function. The correlation length is calculated from the envelope of this autocorrelation function. The instantaneous envelope of a function *f(t)* is defined with eq. (18), where *H(t)* represents the Hilbert transform, eq. (19), of a function *f(t)*.

$$\text{Autocorr}(\mathbf{g},\mathbf{g})_j \Leftrightarrow G_kG_k^*, \qquad k=0,1,2,\ldots length(G)-1, \tag{17}$$

$$A(t)=\sqrt{(f(t))^2+(H(t))^2}\,, \tag{18}$$

$$H(t)=\int_{-\infty}^{+\infty}\frac{1}{\pi\cdot(t-\tau)}\cdot f(\tau)\cdot d\tau\,. \tag{19}$$

The correlation length is calculated from the equivalent strain, eq. (20), and equivalent (Mises) stress, eq. (21). ε_{eq} and σ_{eq} are determined for every Gaussian integration point of the finite elements. For the correlation-length calculation the strains and stresses are assumed to be random variables.

$$\varepsilon_{eq}=\frac{\sqrt{2}}{3}\left[(\varepsilon_x-\varepsilon_y)^2+(\varepsilon_y-\varepsilon_z)^2+(\varepsilon_z-\varepsilon_x)^2+6(\varepsilon_{xy}^2+\varepsilon_{yz}^2+\varepsilon_{zx}^2)\right]^{1/2}, \tag{20}$$

$$\sigma_{eq}=\sqrt{\frac{1}{2}\left[(\sigma_x-\sigma_y)^2+(\sigma_y-\sigma_z)^2+(\sigma_z-\sigma_x)^2+6\tau_{xy}^2+6\tau_{yz}^2+6\tau_{zx}^2\right]}. \tag{21}$$

Since strain and stress are two-dimensional variables, a vector of data for the correlation-length calculation has to be extracted. This can be done in the following way (see Figure 3): i) a point for which the correlation length is to be calculated is selected, ii) a direction α for calculating the correlation length is chosen, iii) the length of the vector is determined by the search radius R, iv) a quadratic two-dimensional interpolation [32] is applied to obtain the values of the strains and stresses in the equally spaced points on the direction line within the search radius (the bold line in Figure 3), v) the correlation length is calculated for the selected direction, vi) the procedure is applied for other directions. The final correlation length is determined as the average value of the correlation lengths for the selected directions. In this study we used six predefined directions: from 0^o up to 150^o in steps of 30^o. The procedure was repeated for every Gaussian point.

The stresses and strains were calculated using the ABAQUS [24] finite-element code. The macroscopic equivalent stress $<\sigma_{eq}>$ and the macroscopic equivalent strain $<\varepsilon_{eq}>$ were calculated as:

$$\left\langle \sigma_{eq} \right\rangle = \frac{1}{V}\int_V \sigma_{eq}\ dV\ ,\ \left\langle \varepsilon_{eq} \right\rangle = \frac{1}{V}\int_V \varepsilon_{eq}\ dV\ , \tag{22}$$

where σ_{eq} stands for the equivalent stress, eq. (21); ε_{eq} for the equivalent strain, eq. (20); and V for the volume of a polycrystalline aggregate.

4 RESULTS AND DISCUSSION

The correlation length is estimated from the strain and stress fields of a finite-element model using 212 crystal grains with a size of 0.4 mm by 0.28 mm. For each Voronoi tessellation models with displacement and stress boundary conditions are analyzed. These models are labeled as d_1, d_2, s_1 and s_2. The letters 'd' and 's' refer to the displacement and stress boundary conditions. The numbers 1 and 2 refer to the 1st and 2nd Voronoi tessellation. When discussing results obtained from the strain or stress fields subscripts 'e' (for ε) and 's' (for σ) are added. All models are loaded with p_1=1400 MPa and $p_2=p_1/2$=700 MPa.

In a previous investigation [33] we determined that the correlation length depends upon the size of a search radius R. Larger search radius would result in higher correlation lengths. At large search radiuses a saturation point is expected where the correlation length would stop increasing and stabilize. However, the computational power for solving such large models is at this time beyond our reach. We determined that the search radius should be larger than the average grain size. In this study we used a search radius R corresponding to twice the average grain size (0.046 mm).

If a small search radius R is chosen, it is possible that the vector **g** will contain insufficient information about the strain and stress fields for a meaningful estimation of the correlation length. On the other hand, when a large search radius R is chosen, the vector **g** contains strain and stress information from a larger 'area', which may not be a representative measure of the local statistics. In addition, when a large search radius R is used, a part of the vector **g** is much more prone to falling outside of the area of the model. For the points of the vector **g** outside of the model area the strains and stresses are assumed to be zero.

4.1 The influence of the Voronoi tessellation

The Voronoi tessellation defines the shape and size of grains. Its influence on calculated correlation lengths can be seen when comparing Figure 5 with Figure 6 (displacement boundary conditions). One can see that shapes of the correlation length curves are similar. As long as the specimen is stressed below the yield point the correlation length does not change. This is in accordance with the statistical theory since the proportional change in the observed strain and/or stress field (e.g. by a factor 1.1) does not change the correlation length. The difference between the correlation lengths calculated from the strain and stress fields is, however, higher for the 1st Voronoi tessellation (0.0014 versus 0.0005 if stressed below the yield point).

Similar observation can be made when comparing the influence of the Voronoi tessellation on the cases with stress boundary conditions, see Figure 7 and Figure 8. The shapes of the correlation length curves are very similar, however, the difference

between the correlation lengths calculated from the strain and stress fields is in this case higher for the 2nd Voronoi tessellation (0.0003 versus 0.0016 if stressed below the yield point).

From the presented cases it can be concluded that the Voronoi tessellation affects the level of the correlation length but has little effect on the shape of its curve.

4.2 The influence of boundary conditions

Boundary conditions affect calculated strain and stress fields and therefore also have an impact on the correlation length. For the same macroscopic equivalent strain a model with displacement boundary conditions will have larger macroscopic equivalent stress than a model with stress boundary conditions. If one wants to assess the effect of boundary conditions on the correlation length, cases with the same Voronoi tessellation have to be compared.

The difference between Figure 5 and Figure 7 is in the boundary condition. For both cases the Voronoi tessellation (1st), material orientations and loads are the same. One can observe that the shapes of the correlation length curves between the two cases are very similar. The largest difference between the two cases is 7.2% for the correlation length calculated from the strain fields and 7.8% for the correlation length calculated from the stress fields. However, for displacement boundary condition the correlation length calculated from the stress field is higher when the specimen is stresses below the yield point. This is not the case with stress boundary conditions. Here the correlation

length calculated from the strain field is higher. Similar conclusions can be made for the 2nd Voronoi tessellation, compare Figure 6 and Figure 8.

Boundary conditions also affect the general level of the correlation lengths calculated from the strain and stress fields. As long as the specimen is stressed below the yield point this difference is larger for displacement boundary condition than for the stress boundary condition (1st Voronoi tessellation). For the 2nd Voronoi tessellation situation is opposite.

From the presented cases it can be concluded that the two boundary conditions have a similar impact as the Voronoi tessellation. Boundary conditions affect the level of the correlation length but have little effect on the shape of its curve.

4.3 General discussion

The selection of strain or stress as a basis for the calculation of the correlation length strongly influences the shape of the correlation length curve. This can be seen in all analyzed cases. If displacement boundary conditions are used, the correlation length calculated from strain field is lower then the one calculated from the stress field (as long as the specimen is stressed below the yield point). Opposite is true if stress boundary conditions are applied. The behavior of the correlation length can, however, be classified into three regions. The first region is when the specimen is stressed below the yield point. There is a difference in correlation lengths calculated from the strain and stress fields, however, this difference and the correlation length in this regions remain

constant. Using this property one can estimate how high must the macroscopic equivalent stress be for first plastic deformations to occur. For the material involved this is estimated at 245 MPa.

The second region begins when the load is increased and the specimens are stressed above the macroscopic yield point. The correlation length starts to decrease. The rate of decrease is different if correlation length is calculated from strain or stress field. In the case of the correlation length calculated from the stress field it can even slightly increase. At this loads first shear bands start to form. It was observed that in some cases (correlation length calculated from the strain field) the areas of higher correlation lengths coincide with the shear bands, see Figure 9 and Figure 10. The grain boundaries are plotted with black (Figure 9) and white lines (Figure 10). A further increase in the load caused widening and elongation of the shear bands. In this region the correlation lengths increased in all analyzed cases.

The last region begins at macroscopic equivalent stress of ≈570 MPa. At this load the correlation length calculated from the strain field starts to decrease. The correlation length calculated from the stress field is still slightly increasing (displacement boundary conditions) or stabilizes (stress boundary conditions) at approximately 0.025 (1^{st} Voronoi tessellation) and 0.022 mm (2^{nd} Voronoi tessellation).

5 CONCLUSIONS

In this study the correlation length for a mesoscopic model of a polycrystalline material has been calculated. By using the correlation length we were able to determine the

length scale of the inhomogeneities. This is an important material property in advanced macroscopic material models.

The calculated strain and stress fields were used to estimate the correlation lengths. The influence of the random grain geometry (Voronoi tessellations) and boundary conditions on the correlation length was estimated. We determined that the Voronoi tessellations and the boundary conditions affect the general level of the correlation length but have little impact on the shape of the correlation length curve. When using displacement boundary conditions, the average correlation lengths calculated from the stress field are, in general, higher than the ones calculated from the strain field. The opposite is true for the stress boundary conditions.

The correlation lengths also depend on the macroscopic load. For elastically deformed polycrystal, the grain's domain of influence is slightly larger than the average grain size. Increasing the macroscopic equivalent stresses between 270 MPa and 500 MPa causes some fluctuations of the domain of influence. With further increase of the macroscopic load, the correlation length calculated from the stress fields reaches its peak value and then decreases continuously.

The calculated correlation lengths were averaged over different directions. This effectively reduced their potential for detecting direction-dependant structures in an anisotropic material. This drawback may be effectively overcome by calculating a two-dimensional autocorrelation function. This represents an important goal for the future work.

Acknowledgments

This work was financially supported in part by the Slovene Ministry of Education, Science and sport and in part by the Nuclear Power plant Krško through the research project L2-5336-0106-03.

6 REFERENCES

[1] S. Suresh, Fatigue of materials, Cambridge University Press, New York, NY, 1991, p.7.

[2] Y. M., Wang, K. Wang, D. Pan, K. Lu, K.J. Hemker, E. Ma, Scripta Materialia, 48 (2003) 1581.

[3] D. J. Kim, T. W. Ku, B. S. Kang, Journal of Materials Processing Technology, 130-131 (2002) 456.

[4] M. Kovač, I. Simonovski, L. Cizelj, Estimating Minimum Polycrystalline Aggregate Size for Macroscopic Material Homogeneity, Proceedings of the International Conference Nuclear Energy for New Europe, September 2002, Kranjska Gora, Slovenia.

[5] C. Rocco, G. V. Guinea, J. Planas, M. Elices, Material and structures, 32 (1999) 210.

[6] B. Jiang, G. J. Weng , Journal of the Mechanics and Physics of Solids, in press.

[7] H. H. Fu, D. J. Benson, M. A. Meyers, Acta Materialia, 49 (2001) 2567.

[8] V. S. Deshpande, A. Needleman, E. Van der Giessen, Acta Materialia 51 (2002) 1.

[9] L. Luo, P. Bowen, P., International Journal of Fatigue, 26 (2004) 113.

[10] A. Echeverría, J. M. Rodriguez-Ibabe, Materials Science and Engineering A, 346 (2003) 149.

[11] P. B. Zdenek, International Journal of Solids and Structures, 37 (2000) 69.

[12] J. Y Cho, J. A. Szpunar, Textures Of Materials, Pts 1 And 2 Materials Science Forum, 408 (2002) 1365.

[13] E. C. Aifantis, International Journal of Engineering Science, 30 (1992) 1279.

[14] J. W. Hutchinson, International Journal of Solids and Structures, 37 (2000) 225.

[15] Y. Huang, S. Qu, K. C. Hwang, M. Li, H. Gao, International Journal of Plasticity, in press.

[16] A. L. Gurson, Plastic Flow and Fracture Behavior of Ductile Materials Incorporating Void Nucleation, Growth and Interaction, PhD dissertation, Brown University, 1975.

[17] V. Tvergaard, International Journal of Fracture, 18 (1982) 237.

[18] Kovač, M., Influence of Microstructure on Development of Large Deformations in Reactor Pressure Vessel Steel, draft of Ph.D. dissertation, University of Ljubljana, 2003.

[19] D. Krajcinovic, M. Vujosevic, International Journal Of Solids And Structures, 35 (1998) 4147.

[20] A. Borbély, H. Biermann, O. Hartmann, Material Science and Engineering A, 313 (2001) 34.

[21] W. Han, A. Eckschlager, H. J. Böhm, Composites Science and Technology, 61 (2001) 1581.

[22] S. Chakraborty, S. S. Dey, Computers & Structures, 55 (1995) 41.

[23] C. A. Schenk, I. R. Schuëller, International Journal of Non-Linear Mechanics, 38 (2003) 1119.

[24] ABAQUS/Standard, Version 6.3-1, Hibbit, Karlsson & Sorensen Inc., 2002.

[25] S. Nemat-Nasser, M. Hori, Micromechanics: Overall Properties of Heterogeneous Materials, Elsevier Science B. V, Amsterdam, 1993, p. 75.

[26] F. Aurenhammer, ACM Computing Surveys, 23 (1991) 345.

[27] O. Watanabe, H. M. Zbib, E. Takenouchi, International Journal of Plasticity, 14 (1998), 771.

[28] M. Kovač, L. Cizelj, International Journal of Plasticity, submitted for publication.

[29] G. Grimvall, Thermophysical Properties of Materials, Elsevier Science B. V, Amsterdam, 1999, p. 38.

[30] A. Needleman, Acta Materialia, 48 (2000) 105.

[31] D. Peirce, R. J. Asaro, A. Needleman, Acta metallurgica, 31 (1983) 1951.

[32] R. J. Renka, ACM Transactions on Mathematical Software, 14 (1988) 139.

[33] I. Simonovski, M. Kovač, L. Cizelj, Correlation Length Estimation Issues In Stochastic Material Model, Proceedings of the 17th International Conference on Structural Mechanics in Reactor Technology (SMiRT 17), August 2003, Prague, Czech Republic.

Figures

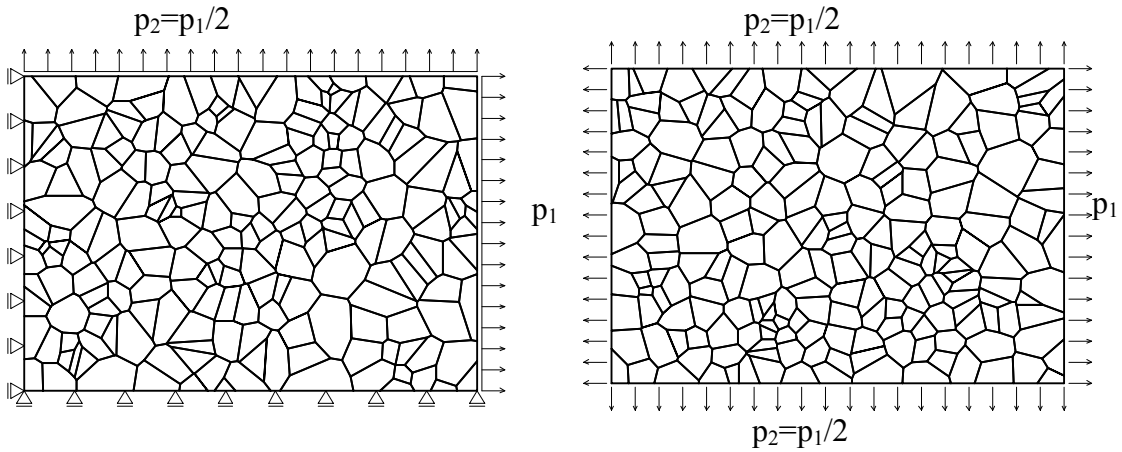

Figure 1

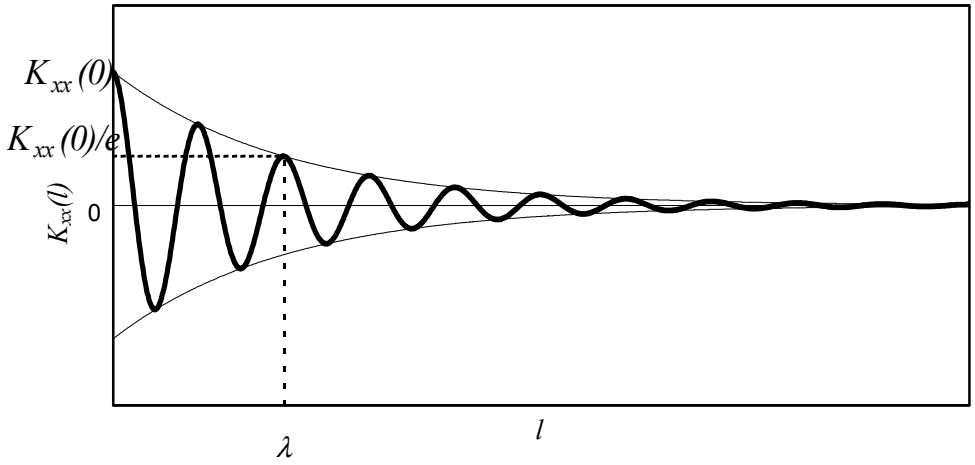

Figure 2

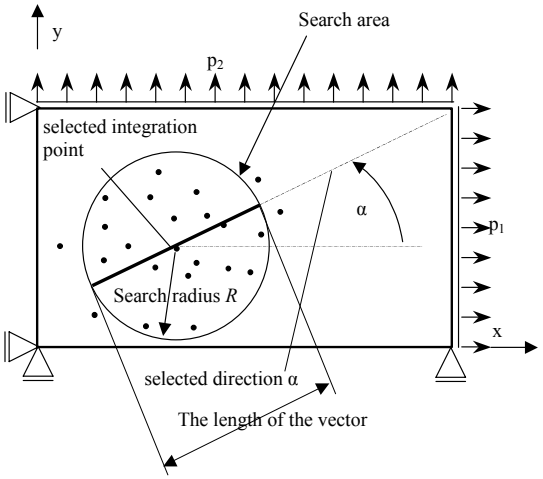

Figure 3

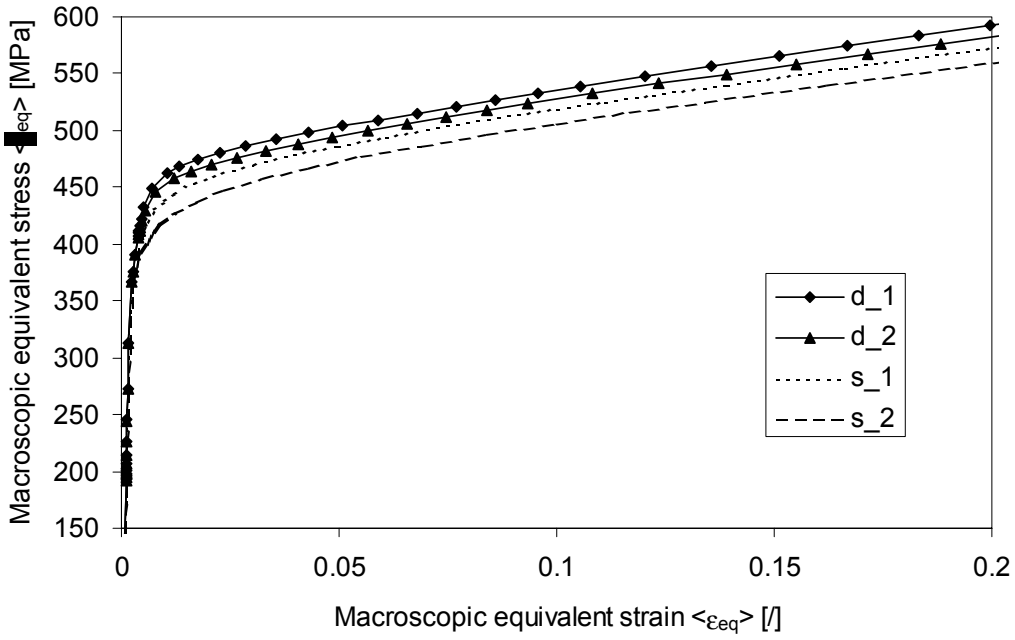

Figure 4

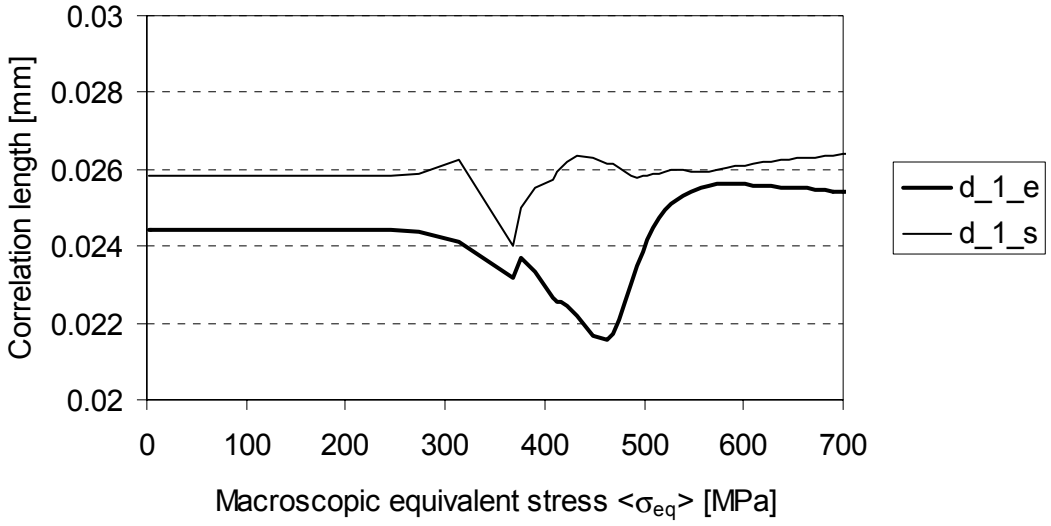

Figure 5

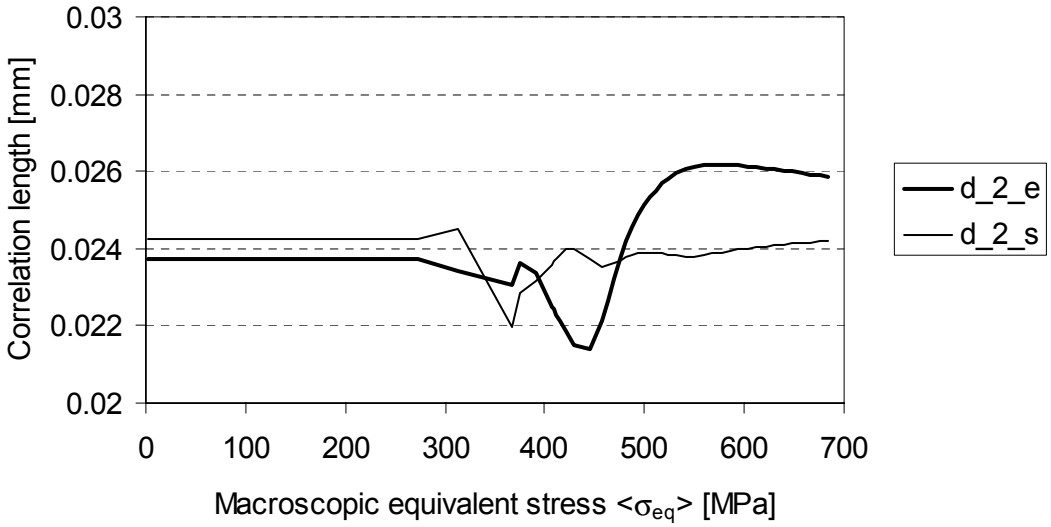

Figure 6

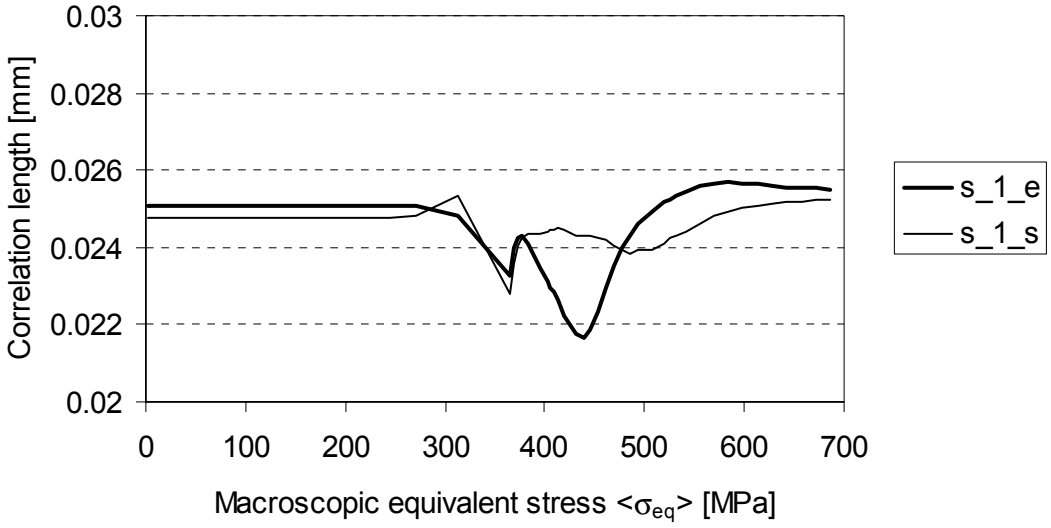

Figure 7

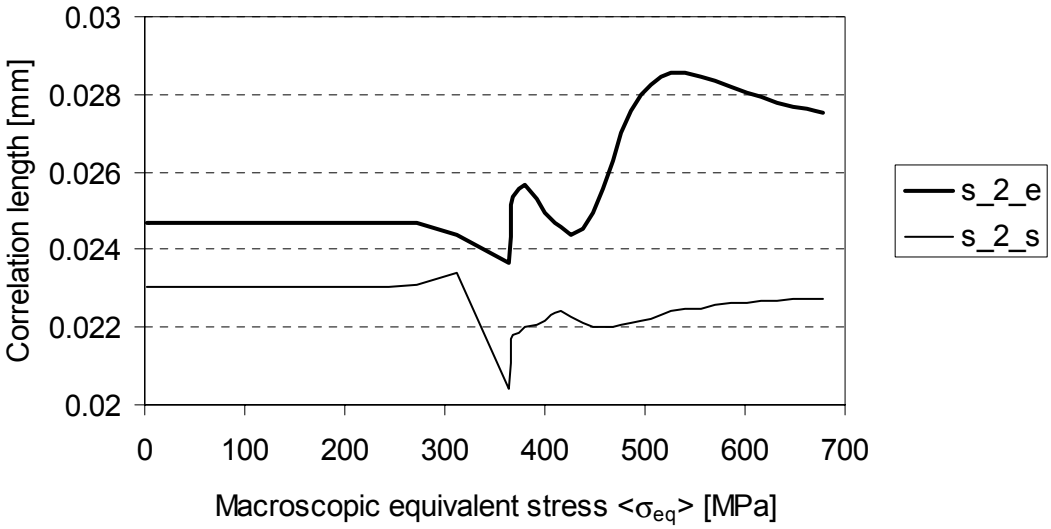

Figure 8

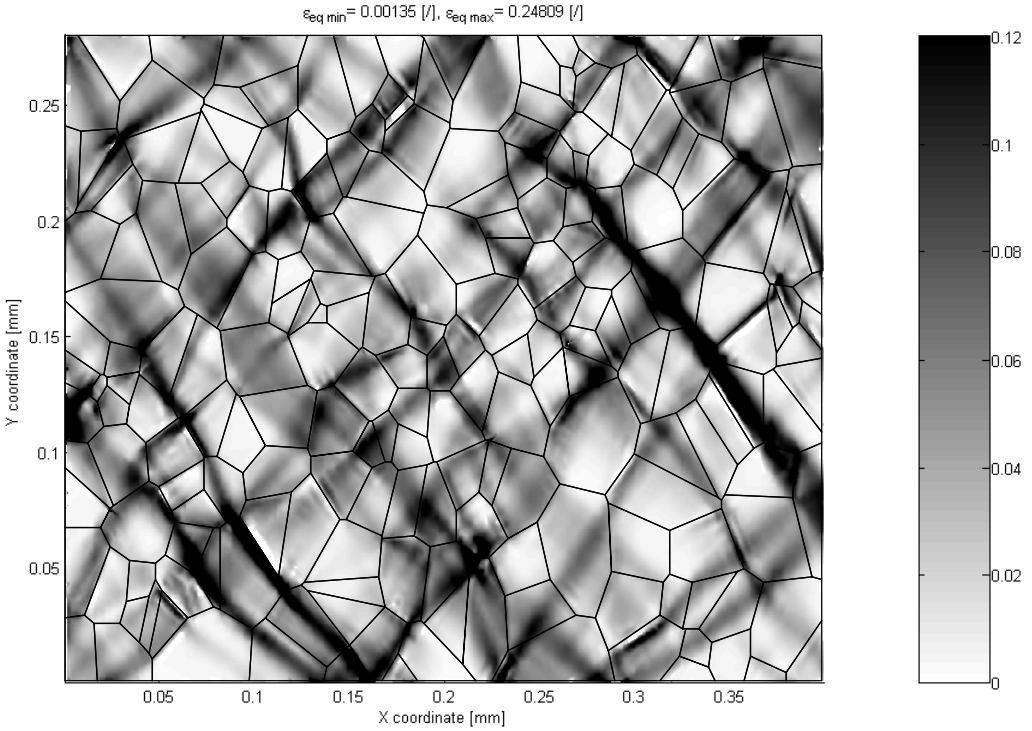

Figure 9

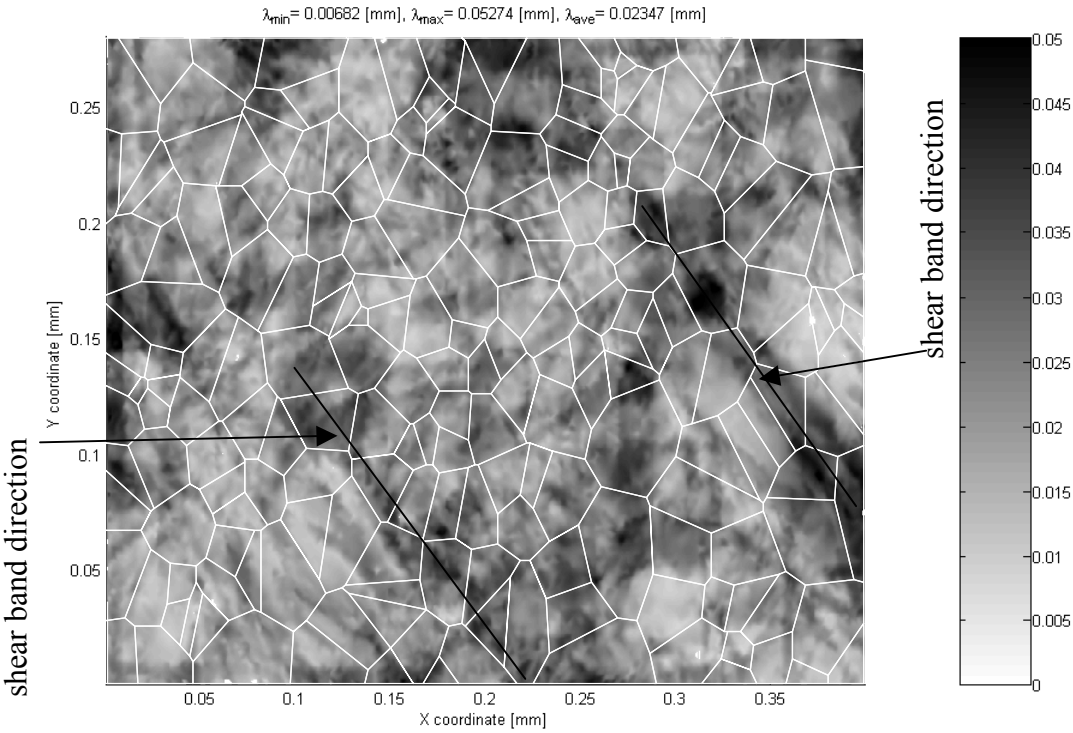

Figure 10

Tables

Table 1

1st Voronoi tessellation			
	Edge length [mm]	Edge number [/]	Grain area [mm^2]
Average value	0.0923	4.76	0.000528
Standard deviation	0.0249	1.24	0.000297

2nd Voronoi tessellation			
	Edge length [mm]	Edge number [/]	Grain area [mm^2]
Average value	0.0919	4.75	0.000528
Standard deviation	0.0219	1.22	0.000268

List of Tables

List of Figures

Figure 9: Equivalent strain ε_{eq}; $<\varepsilon_{eq}>$= 0.035, $<\sigma_{eq}>$= 492.12 MPa . Displacement boundary conditions, 1st Voronoi tessellation

Figure 10: Correlation length at $<\varepsilon_{eq}>$= 0.035, $<\sigma_{eq}>$= 492.12 MPa . Displacement boundary conditions, 1st Voronoi tessellation